JOURNAL OF ELECTROMAGNETIC ENGINEERING AND SCIENCE, VOL. 15, NO. 2, 97~103, APR. 2015

http://dx.doi.org/10.5515/JKIEES.2015.15.2.97
ISSN 2234-8395 (Online) · ISSN 2234-8409 (Print)

Analysis of Absorption Loss by a Human Body in On-to-Off Body Communication at 2.45 GHz

Jaesung Jeon · Sangwoo Lee · Jaehoon Choi · Sunwoo Kim*

Abstract

This paper investigates the effect of absorption loss by a human body to the received signal strength with respect to on-body transmitting antenna positions in on-to-off wireless body area networks. This investigation is based on measurement results obtained from experiments performed on human bodies (male and female) using planar inverted-F antennas in an anechoic chamber. The total absorption loss by the human body is also presented through the SEMCAD-X simulations. Our investigation showed that the received signal strength becomes lower when the transmitting antenna is mounted at a specific position where more absorption loss is experienced. The statistical analyses of on-to-off body channel characteristics based on the measurement results are presented.

Key Words: Absorption Loss, Channel Characterization, Off-Body System, Received Signal Strength.

I. INTRODUCTION

Wireless body area networks (WBANs) have received a great deal of attention for facilitation of different applications including healthcare, sport activities, and personal assistance. These applications involve on-to-off body communication scenarios where physiological and activity data from a person are sent to the monitoring server. In such scenarios, the radio signal is affected by environmental factors as well as by human body (e.g., movements, structures, and tissues, etc.). As a result, typical wireless channel models do not fit well with WBAN environments.

For several years, many efforts have been made to identify the propagation characteristics in on-to-off body communication [1−4]. In indoor environments, the log-normal and Rayleigh distributions provide good fit to the on-to-off body channels for standing and for walking, respectively [1]. Smith et al. [2] showed that the on-to-off body channels for sleeping persons follow the Gamma distribution. The variation in the channel characteristic with the blockage of the line-of-sight path by the human body (i.e., shadowing effect) was investigated in [3]. A new statistical channel model for the path blockage was also introduced in [4]. Other investigations of the on-to-off body channel characteristics can be found in [5, 6].

The channel characteristics, in fact, depend on various factors such as the environments, subjects (gender and body morphology), types, and positions of the antennas in addition to the body activities [7, 8]. However, with the implicit assumption that the effects of the other factors are relatively negligible, the previous investigations focused on how the propagation channel characteristics change according to the body movements. Based on our preliminary experimental results, the on-to-off body channel characteristics vary considerably due to the transmitting antenna positions on the body while the other conditions are fixed. Efforts are ongo-

Manuscript received December 19, 2014 ; Revised April 2, 2015 ; Accepted April 7, 2015. (ID No. 20141219-070J)
Department of Electronics and Computer Engineering, Hanyang University, Seoul, Korea.
*Corresponding Author: Sunwoo Kim (e-mail: remero@hanyang.ac.kr)

ing to investigate the effects of antenna positions on the on-body channels [8], but to the best of our knowledge, no substantial propagation characterization and analysis of the on-to-off body channel has been conducted with respect to the antenna positions.

Recent experimental results (see [9] and references therein) showed that the power absorption is a dominant factor influencing the WBAN performance. Motivated by these results, we investigate the effect of body absorption losses (ALs) on the on-to-off body channel characteristic in this paper. The received signal strength (RSS) and the ALs are measured with respect to the on-body transmitting antenna positions through experiments and simulations. A statistical analysis is presented to characterize the on-to-off body channels as a function of the on-body transmitting antenna positions.

The rest of this paper is organized as follows. Section II describes the measurement setup and the power loss model. Section III analyzes the effect of the body AL on the on-to-off body channel with experimental and simulation results. Section IV concludes this paper.

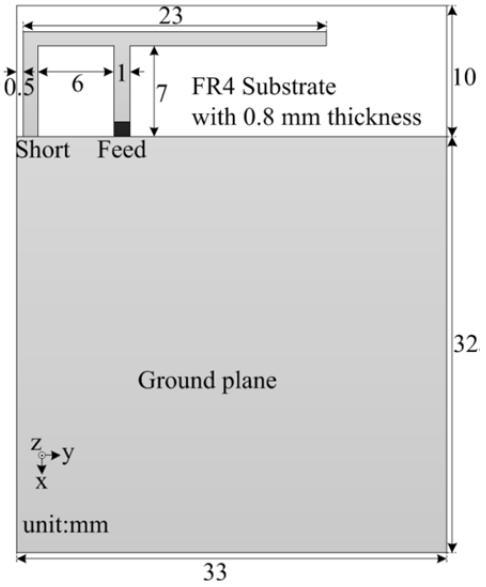

(a)

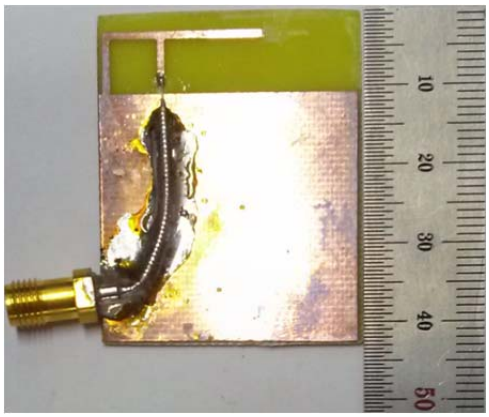

(b)

Fig. 1. Planar inverted-F antenna (PIFA) for experiments. (a) Geometry of PIFA and (b) fabricated PIFA.

II. Experimental Procedure

1. Measurement Setup

The measurement system consisted of a transmitting/receiving (Tx/Rx) pair of planar inverted-F antennas (PIFAs) and a vector network analyzer (VNA; Rohde & Schwarz ZVB20, Germany). Fig. 1 shows the geometry of the PIFA. The PIFA is designed on a FR4 substrate with a relative permittivity of 4.4, and the total size of the substrate is 33×42 mm^2. The antenna has a dimension of $23\times8\times0.8$ mm^3. The PIFAs operated in the 2.45 GHz ISM band have an omnidirectional radiation pattern in free space (Fig. 2(a)) and have a directional pattern when mounted on the body (Fig. 2(b)).

A schematic diagram of the measurement setup is shown in Fig. 3. The Tx antenna was placed at one of three positions (ℓ_1, ℓ_2, ℓ_3) on the body, as shown in Fig. 3. ℓ_1 is the position of the heart, ℓ_2 is the position of the right upper-chest, and ℓ_3 is the position of the navel. The Rx

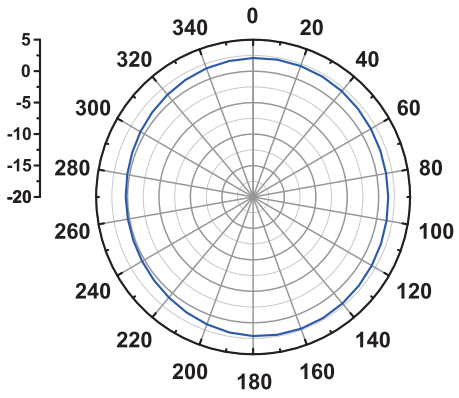

(a)

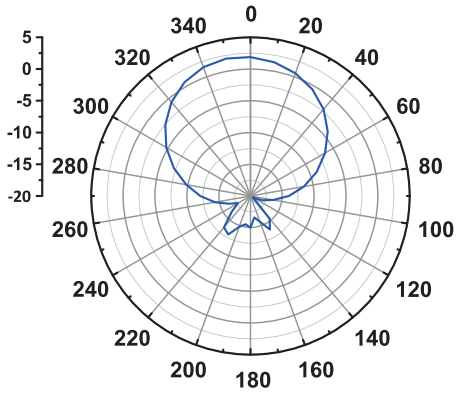

(b)

Fig. 2. Radiation pattern of planar inverted-F antenna: (a) free space and (b) on-body.

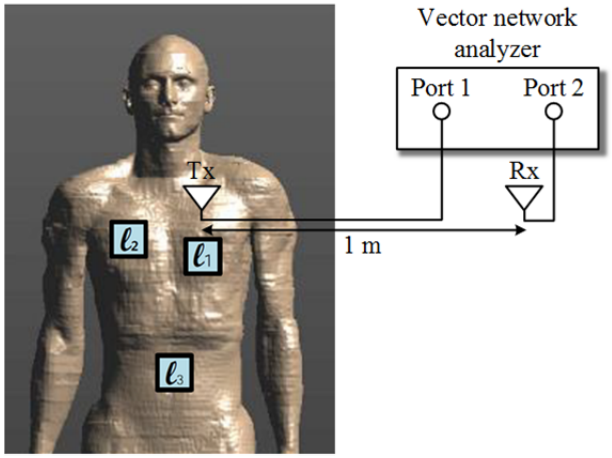

Fig. 3. Measurement setup for on-to-off body communication.

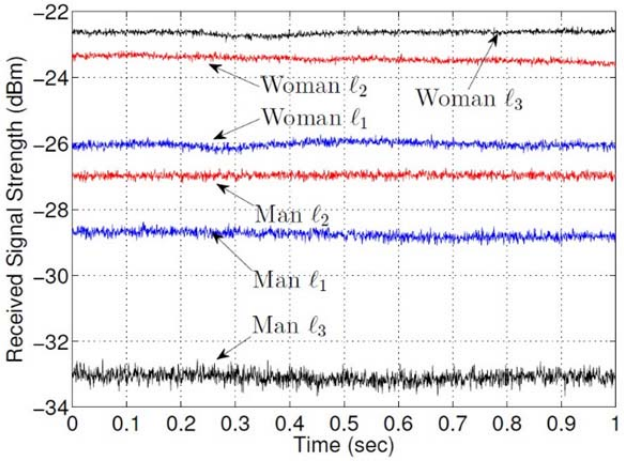

Fig. 4. Measured received signal strength at each Tx antenna position.

antenna was placed 1 m away from the body, at the same height as the Tx antenna. Hence, the path loss was assumed to be constant regardless of the Tx antenna positions. The VNA generated a continuous wave signal of 0 dBm (1 mW) and sent a continuous wave signal through the Tx antenna at the 2.45 GHz ISM band. The VNA also operated in a single trace and single frequency mode to measure RSS in the time-domain. In a sweep time of 1 second, 1,601 samples were recorded for each Tx antenna position. The experiments were conducted on the body of a 1.76 m/73 kg male subject and a 1.60 m/50 kg female subject, standing motionless in an anechoic chamber. For the real experiments, the Tx antenna was attached to the skin, but a gap with a thickness less than 1 cm could occur due to the body morphology. The effects of multipath, fading, and shadowing from the human actions were neglected in the experiments. For each setting, 10 experiments were carried out. The SEMCAD-X simulations used the Duke model (1.77 m/72 kg) and Ella model (1.63 m/58 kg). The simulation settings were identical to those of the real experiments.

2. Theoretical Background

Consider a WBAN system in which a Tx antenna is mounted on ℓ_i and transmits a signal with a power of P_{Tx}. The RSS at the Rx antenna can then be expressed as

$$P_{\mathrm{Rx}}(d,\ell_i) = P_{\mathrm{Tx}} - P_{\mathrm{PL}}(d) - P_{\alpha}(d,\ell_i) - P_{\mathrm{AL}}(\ell_i) \qquad (1)$$

where d is the Tx-Rx distance separation, $P_{\mathrm{PL}}(d)$ is the path loss, $P_{\alpha}(d,\ell_i)$ is the environmental loss by multipath, fading, and shadowing, and $P_{\mathrm{AL}}(\ell_i)$ is the body AL when the Tx antenna is mounted on ℓ_i. In our measurement system, as the Tx-Rx distance is fixed to $d = 1$ m, and the human subjects are standing motionless in an anechoic chamber, the path loss $P_{\mathrm{PL}}(d)$ is considered constant and the environmental loss $P_{\alpha}(d,\ell_i)$ is assumed to be negligibly small. Hence, (1) can be approximated as

$$P_{\mathrm{Rx}}(d,\ell_i) \approx P_0 - P_{\mathrm{AL}}(\ell_i) = P_{\mathrm{Rx}}(\ell_i) \qquad (2)$$

where $P_0 = P_{\mathrm{Tx}} - P_{\mathrm{PL}}(d)$, and it is assumed to be constant regardless of the Tx antenna positions. From (2), we intuitively know that the RSS is dependent on the body AL $P_{\mathrm{AL}}(\ell_i)$.

III. Analysis of Body Absorption Loss

1. Received Signal Strength and Body Absorption Loss

The time-domain results of RSS measurements for the male and female subjects are shown in Fig. 4. The RSS can differ according to the Tx antenna positions. In the case of the male subject, RSS at ℓ_2 is higher than that at ℓ_3 by around 7 dB (Note that RSS at ℓ_i says that a value is measured at the Rx antenna when the Tx antenna is located at ℓ_i on the body). For the female subject, the largest difference between the RSS measurements with respect to the Tx antenna positions is approximately 3.5 dB. The average value of the RSS measurements is given with the simulation results and the AL in Table 1. The body AL $P_{\mathrm{AL}}(\ell_i)$ for each Tx antenna position ℓ_i was measured with SEM-

Table 1. Experiment and simulation results

Subject	Tx antenna position	Measured RSS (dBm)	Simulated RSS (dBm)	AL (mW)
Male	ℓ_1	−28.7645	−38.8	0.687
	ℓ_2	−26.9714	−37.5	0.568
	ℓ_3	−33.0887	−39.3	0.717
Female	ℓ_1	−26.0318	−39.7	0.645
	ℓ_2	−23.4385	−37.8	0.391
	ℓ_3	−22.6468	−37.3	0.540

Tx=transmitting, RSS=received signal strength, AL=absorption loss.

CAD-X simulations. According to Table 1, lower RSS is observed with greater AL, which means more power loss due to the body absorption. We note that the body structures of our subjects and the dielectric properties for tissues may not be same as those in the simulations, although the weights and heights of the subjects are similar to those of the Duke and Ella models.

Hence, the experiment and simulation results can differ. However, the order of RSS values in both experiments and simulations is identical. For the male subject, the lowest RSS is measured in both experiments and simulations when the Tx antenna is mounted on ℓ_3, where a total of 0.717 mW is absorbed. The RSS is found to be highest at ℓ_2, where the body absorption is lowest (0.568 mW). For the female subject, the highest and lowest ALs are observed at ℓ_1 and ℓ_2, respectively. As a result, the lowest RSS is measured when the Tx antenna is mounted on ℓ_1. However, the RSS at ℓ_3 is slightly higher than that at ℓ_2, although $P_{\mathrm{AL}}(\ell_2)$ is lower than $P_{\mathrm{AL}}(\ell_3)$. This is due to the curves on the female subject (body morphology). We will discuss on this in the following subsection.

2. Results and Discussion

The total AL by the human body depends on temperature, frequency, and the dielectric properties of tissues around the Tx antenna [10, 11]. In our investigation, the change in the dielectric properties according to the Tx antenna positions only makes a difference because the effects of temperature and frequency remain constant. Although the temperatures can differ at various body (Tx antenna) positions, note that the AL due to the body temperature is considered constant regardless of the positions since the temperature differences are insignificant. The dielectric properties are defined in terms of relative permittivity ε_r and conductivity σ, and their numerical values for the simulations are described in Table 2. The absorption is well-known to depend more on conductivity than on relative permittivity; namely, as conductivity increases, the AL also increases [12, 13].

We recall that $P_{\mathrm{AL}}(\ell_1)$ =0.687 mW, $P_{\mathrm{AL}}(\ell_2)$ =0.568 mW, and $P_{\mathrm{AL}}(\ell_3)$ =0.717 mW for the male subject. When comparing the body positions ℓ_1 and ℓ_2, the main difference is the existence/absence of the heart. At ℓ_1, there exists the heart. The heart has the dielectric properties of ε_r = 58.3 and σ = 2.54 S/m. Hence, higher conductivity is experienced at ℓ_1 than at ℓ_2. In other words, more AL and higher RSS are observed at ℓ_1 than at ℓ_2. The presence of the small intestine (ε_r = 54.4 and σ = 3.17 S/m) at ℓ_3 results in the highest conductivity. In summary, $\sigma(\ell_3) > \sigma(\ell_1) > \sigma(\ell_2)$ where $\sigma(\ell_i)$ is the conductivity at ℓ_i. As a result, $P_{\mathrm{AL}}(\ell_3) > P_{\mathrm{AL}}(\ell_1) > P_{\mathrm{AL}}(\ell_2)$ and $P_{\mathrm{Rx}}(\ell_2) > P_{\mathrm{Rx}}(\ell_1) > P_{\mathrm{Rx}}(\ell_3)$ are satisfied.

Table 2. Simulated dielectric properties for various tissues

Tissue	Relative permittivity ε_r	Conductivity σ (S/m)
Blood	58.3	2.540
Fat	10.8	0.268
Heart	58.3	2.540
Lungs	20.5	0.804
Muscle	52.7	1.740
Skin	11.4	0.394
Small intestine	54.4	3.170
Breast	57.2	1.970

Different results are obtained for the female subject than for the male subject: $P_{\mathrm{AL}}(\ell_1) > P_{\mathrm{AL}}(\ell_3) > P_{\mathrm{AL}}(\ell_2)$ and $P_{\mathrm{Rx}}(\ell_3) > P_{\mathrm{Rx}}(\ell_2) > P_{\mathrm{Rx}}(\ell_1)$. Unlike the male subject, the female has breasts, which create a small air gap (air internal of σ = 0 S/m) between the Tx antenna and the body surface. This air gap reduces the AL. The effective dielectric constant of the antenna can also vary with the air gap, which also distorts the impedance matching and radiation characteristics of the antenna. These affect RSS in addition to the body AL, and this is the main reason why $P_{\mathrm{Rx}}(\ell_1)$ and $P_{\mathrm{Rx}}(\ell_2)$ are lower than $P_{\mathrm{Rx}}(\ell_3)$ for the female. Unfortunately, it is not easy to measure the variations and to analyze their effects in the time-domain. Note that the body AL is not a function of only the dielectric properties of the human tissues. The AL is also related to the weight and size of each human tissue, their distributions, and the body structures, which will be investigated in future work. This is another reason that explains the differences in the results from the male and female subjects.

The complexity and variety of body structures may preclude the derivation of explicit formulas that compute the body AL and measure its quantitative effect on the RSS. However, our investigation showed that the body AL is a dominant parameter influencing the RSS.

3. Statistical Analysis

For the statistical analysis, all the RSS measurements from each Tx antenna position were normalized such that normalized RSS $\in$ [0,1] dB. The normalized RSS is denoted by $x \in [0,1]$. In order to perform the statistical analysis of the results, the normalized RSS distributions are compared with well-known theoretical distribution models: Normal, Weibull, Gamma, Rician, and Nakagami-m [14]. The parameter estimates of the theoretical distributions are obtained by using the maximum likelihood estimation method. The best fit distribution for each measurement is determined using the Kolmogorov-Smirnov goodness-of-fit test (KS test)

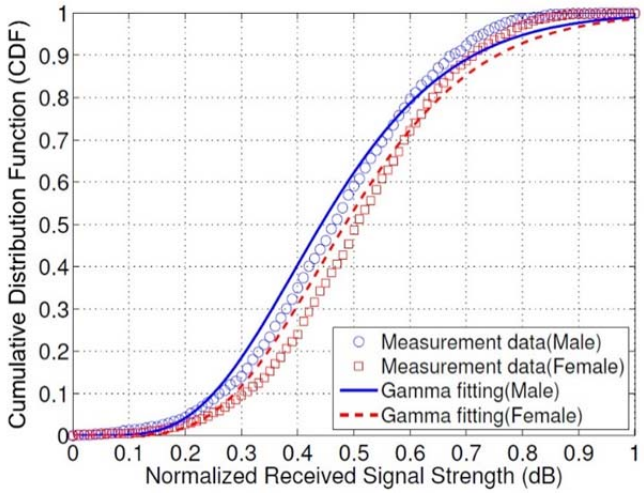

Fig. 5. CDF of normalized received signal strength at Tx antenna position ℓ_1 and best fit Gamma CDF.

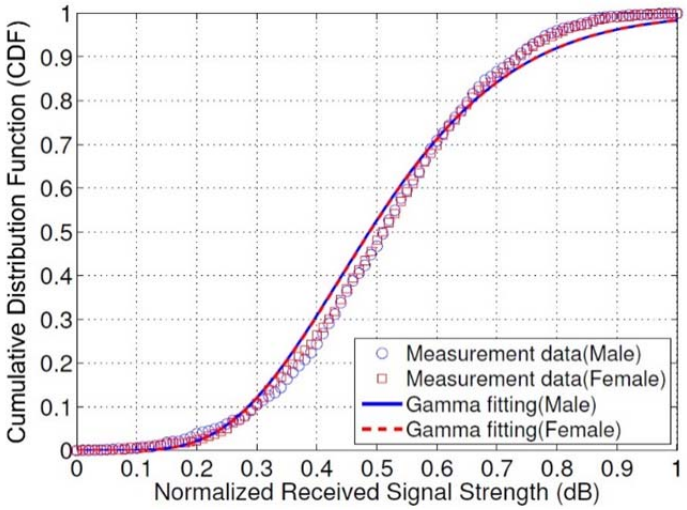

Fig. 6. CDF of normalized received signal strength at Tx antenna position ℓ_2 and best fit Gamma CDF.

[14]. This test calculates the maximum distance between the empirical distribution function (EDF) of the measured data and the cumulative distribution function (CDF) of the theoretical reference model. Among the theoretical models, the one having the minimum distance is selected as the best fit distribution.

The KS statistic is then defined as [14]

$$D = \max_x |F_E(x) - F_X(x)| \tag{3}$$

where $F_E(x)$ is the EDF value of the measured data and $F_X(x)$ is the CDF value of a theoretical reference distribution at $x \in [0,1]$. Table 3 presents the KS statistic values for the five distributions. The KS statistic value is a measure of the fitting error: As the KS statistic value is smaller, the reference distribution provides better fit. In our investigation, the Gamma distribution was the best fitting model. Figs. 5–7 show the EDFs of the measured data and the best fit Gamma distributions for the male and female subjects when the Tx antenna is mounted on ℓ_1, ℓ_2, and ℓ_3.

Meanwhile, the Gamma probability density function is given by

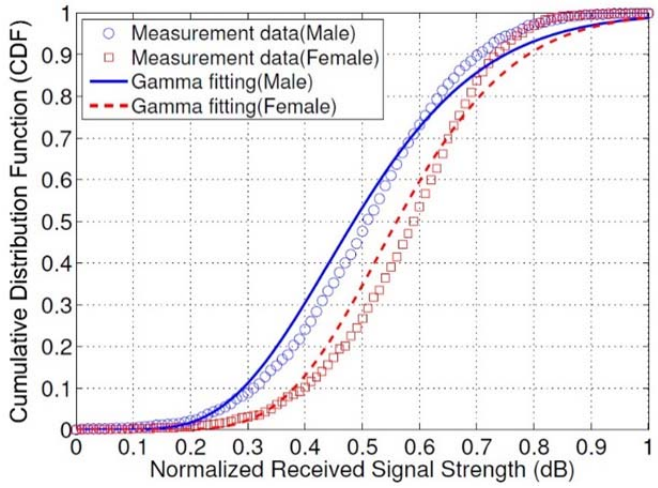

Fig. 7. CDF of normalized received signal strength at Tx antenna position ℓ_3 and best fit Gamma CDF

Table 3. Kolmogorov-Smirnov statistic value and estimated parameters

Type	Male			Female		
	ℓ_1	ℓ_2	ℓ_3	ℓ_1	ℓ_2	ℓ_3
Normal	0.9872	0.9996	0.9997	1.0000	0.9645	0.0664
Weibull	0.8859	0.7016	0.7301	0.7579	0.9936	0.4225
Gamma	**0.0056**	**0.0023**	**0.0012**	**0.0013**	**0.0197**	**0.0001**
Rician	0.9995	0.9967	0.9948	0.9999	0.9886	0.0552
Nakagami-m	0.2119	0.0934	0.0452	0.0714	0.3742	0.0005
Gamma parameter						
a	6.4765	7.2015	7.9090	7.6039	7.2479	13.190
b	0.0719	0.0709	0.0640	0.0666	0.0706	0.0436

$$f_{\text{Gamma}}(x|a,b) = \frac{1}{b^a \Gamma(a)} x^{a-1} e^{\frac{-x}{b}} \quad (4)$$

where a is the fading parameter, b is the scale parameter, and $\Gamma(a)$ is the Gamma function; a and b are referred to as the Gamma parameters. The estimated parameters (a,b) of the Gamma distributions for the male and female subjects at each Tx antenna position are shown in Table 3. We denote the estimates of a and b at ℓ_i by $(a,b|\ell_i)$. For the male subject, $(\mathrm{a},\mathrm{b}|\ell_1) = (6.4765,\ 0.0719)$ at ℓ_1, $(\mathrm{a},\mathrm{b}|\ell_2) = (7.2015,\ 0.0709)$ at ℓ_2, and $(\mathrm{a},\mathrm{b}|\ell_3) = (7.9090,\ 0.0640)$ at ℓ_3. For the female subject with respect to the Tx antenna positions, $(\mathrm{a},\mathrm{b}|\ell_1) =$ at $(7.6039,\ 0.0666)$ ℓ_1, $(\mathrm{a},\mathrm{b}|\ell_2) = (7.2479,\ 0.0706)$ at ℓ_2, and $(\mathrm{a},\mathrm{b}|\ell_3) = (13.190,\ 0.0436)$ at ℓ_3.

IV. Conclusions

This paper investigates the on-to-off body channel characteristics at 2.45 GHz with respect to different Tx antenna positions. The experiments and simulations confirmed that different channel characteristics are observed according to the on-body Tx antenna positions and that they are dependent on the AL generated by the human body. Moreover, due to the differences in the body morphology and structure, we observed that the male and female subjects have considerably different channel characteristics. Statistical analyses were performed by comparing the measurement data to the theoretical reference distribution models. For all measurement sets, the Gamma distribution function provided the best fit to the experimental data. Our experimental results can serve as a good reference for future work on the on-to-off body channel characteristics, taking into account the effects of the antenna positions and the body AL. However, these results are presented only as guidelines since human beings have different body sizes, body structures, and body shapes, which need to be further investigated.

This work was supported by the National Research Foundation of Korea (NRF) grant funded by the Korea government (No. 2010-0017934, NRF-2013R1A1A206-2728).

References

[1] D. Smith, L. Hanlen, J. Zhang, D. Miniutti, D. Rodda, and B. Gilbert, "Characterization of the dynamic narrowband on-body to off-body area channel," in *Proceedings of IEEE International Conference on Communications (ICC'09)*, Dresden, Germany, 2009, pp. 1−6.

[2] D. B. Smith, D. Miniutti, and L. W. Hanlen, "Characterization of the body-area propagation channel for monitoring a subject sleeping," *IEEE Transactions on Antennas and Propagation*, vol. 59, no. 11, pp. 4388−4392, 2011.

[3] S. L. Cotton, A. McKernan, A. J. Ali, and W. G. Scanlon, "An experimental study on the impact of human body shadowing in off-body communications channels at 2.45 GHz," in *Proceedings of the 5th European Conference on Antennas and Propagation (EUCAP),* Rome, Italy, 2011, pp. 3133−3137.

[4] S. L. Cotton, "A statistical model for shadowed body-centric communications channels: theory and validation," *IEEE Transactions on Antennas and Propagation*, vol. 62, no. 3, pp. 1416−1424, 2014.

[5] R. Rosini and R. D'Errico, "Off-body channel modelling at 2.45 GHz for two different antennas," in *Proceedings of the 6th European Conference on Antennas and Propagation (EUCAP)*, Prague, Czech Republic, 2012, pp. 3378−3382.

[6] R. Rosini and R. D'Errico, "Space-time correlation for on-to-off body channels at 2.45 GHz," in *Proceedings of the 7th European Conference on Antennas and Propagation (EuCAP)*, Gothenburg, Germany, 2013, pp. 3529−3533.

[7] M. O. Munoz, R. Foster, and Y. Hao, "On-body channel measurement using wireless sensors," *IEEE Transactions on Antennas and Propagation*, vol. 60, no. 7, pp. 3397−3406, 2012.

[8] A. Michalopoulou, A. A. Alexandridis, K. Peppas, T. Zervos, F. Lazarakis, K. Dangakis, and D. I. Kaklamani, "Statistical analysis for on-body spatial diversity communications at 2.45 GHz," *IEEE Transactions on Antennas and Propagation*, vol. 60, no. 8, pp. 4014−4019, 2012.

[9] D. Kurup, W. Joseph, G. Vermeeren, and L. Martens, "Specific absorption rate and path loss in specific body location in heterogeneous human model," *IET Microwaves, Antennas & Propagation*, vol. 7, no. 1, pp. 35−43, 2013.

[10] X. Liu, H. J. Chen, Y. Alfadhl, X. Chen, C. Parini, and D. Wen, "Conductivity and frequency dependent specific absorption rate," *Journal of Applied Physics*, vol. 113, no. 7, article id. 074902, 2013.

[11] N. Ticaud, S. Kohler, P. Jarrige, L. Duvillaret, G. Gaborit, R. P. O'Connor, D. Arnaud-Cormos, and P. Leveque, "Specific absorption rate assessment using simultaneous electric field and temperature measurements," *IEEE Antennas and Wireless Propagation Letters*, vol. 11, pp. 252−255, 2012.

[12] P. Gajsek, W. D. Hurt, J. M. Ziriax, and P. A. Mason, "Parametric dependence of SAR on permittivity values in a man model," *IEEE Transactions on Biomedical Engineering*, vol. 48, no. 10, pp. 1169−1177, 2001.
[13] W. D. Hurt, J. M. Ziriax, and P. A. Mason, "Variability in EMF permittivity values: implications for SAR calculations," *IEEE Transactions on Biomedical Engineering*, vol. 47, no. 3, pp. 396−401, 2000.
[14] A. Michalopoulou, A. A. Alexandridis, K. Peppas, T. Zervos, F. Lazarakis, K. Dangakis, and D. Kaklamani, "On-body channel statistical analysis based on measurements in an indoor environment at 2.45 GHz," *IET Microwaves, Antennas & Propagation*, vol. 6, no. 6, pp. 636−645, 2012.

Jaesung Jeon
received a B.S. degree in Electrical Engineering from Soongsil University, Seoul, Korea in 2012. He received the M.S. degree in Electronics and Computer Engineering from Hanyang University, Seoul, Korea in 2014.

Jaehoon Choi

received a B.S. degree from Hanyang University, Korea, an M.S. degree and a Ph.D. degree from Ohio State University, Ohio, in 1980, 1986, and 1989, respectively. From 1989-1991, he was a research analyst with the Telecommunication Research Center at Arizona State University, Tempe, Arizona. He worked for Korea Telecom as a team leader of the Satellite Communication Division from 1991 to 1995. Since 1995, he has been a professor in the Department of Electronics and Computer Engineering at Hanyang University, Korea. He has published more than 100 refereed journal articles and numerous conference proceedings. He also holds over 20 patents. His research interests include antennas, microwave circuit design, and EMC. Currently, his research is mainly focused on the design of compact, multi-band antennas for mobile wireless communication, software defined radio (SDR) systems, and ultra-wideband (UWB) systems.

Sangwoo Lee

received B.S. and M.S. degrees, both in Electrical Engineering, from Ajou University, Suwon, Korea in 2009 and 2011, respectively. He is currently pursuing a Ph.D. degree in Electronics and Computer Engineering at Hanyang University, Seoul, Korea.

Sunwoo Kim

received a B.S. in Electrical Engineering from Hanyang University, Seoul, Korea in 1999, and M.S. and Ph.D. degrees in Electrical and Computer Engineering from the University of California, Santa Barbara, CA in 2002 and 2005, respectively. He is currently an associate professor in the Department of Electronics Engineering, Hanyang University, Seoul, Korea.